ELSEVIER

7 October 1996

PHYSICS LETTERS A

Physics Letters A 221 (1996) 343–349

Complex-temperature phase diagram of the 1D Z_6 clock model and its connection with higher-dimensional models

Victor Matveev [1], Robert Shrock [2]

Institute for Theoretical Physics, State University of New York, Stony Brook, NY 11794-3840, USA

Received 3 June 1996; accepted for publication 26 July 1996
Communicated by A.R. Bishop

Abstract

We determine the exact complex-temperature (CT) phase diagram of the 1D Z_6 clock model. This is of interest because it is the first exactly solved system with a CT phase boundary exhibiting a finite-K intersection point where an odd number of curves (namely, three) meet, and yields a deeper insight into this phenomenon. Such intersection points occur in the 3D spin 1/2 Ising model and appear to occur in the 2D spin 1 Ising model. Further, extending our earlier work on the higher-spin Ising model, we point out an intriguing connection between the CT phase diagrams for the 1D and 2D Z_6 clock models.

We report here a determination of the exact complex-temperature phase diagram for the 1D Z_6 clock model and show how the results give a deeper insight into certain features of higher-dimensional models. The idea of generalizing a variable, on which the free energy depends, from real physical values to complex values was pioneered by Yang and Lee [1], who carried this out for the external magnetic field and proved a celebrated circle theorem on the complex-field zeros of the Ising model partition function. The generalization of temperature to complex values, performed first for the Ising model [2], has also been quite fruitful, since it enables one to understand better the behavior of various thermodynamic quantities as analytic functions of complex temperature (CT) and to see how physical phases of a given model generalize to regions in CT variables. Indeed, a knowledge of the complex-temperature phase diagram of a model for which the free energy is not known provides further constraints to guide progress toward an exact solution. A classic example relevant here is the 3D Ising model; the main purpose of the present work is to present some exact results for a 1D model which elucidate an important feature of the complex-temperature phase diagram of the 3D Ising model. Some early works on CT singularities include Refs. [3–6] studying partition function zeros, and Ref. [7], motivated by the effect of these singularities on low-temperature series. The continuous locus of points in the complex-temperature plane where the free energy is non-analytic is denoted $\mathcal{B}$. For the spin models of interest here, with isotropic, nearest-neighbor spin–spin couplings, this is a 1-dimensional curve (including possible line segments). Parts of $\mathcal{B}$ form boundaries of various regions, some of which are complex-temperature extensions of physical phases and some of which may have no overlap with any

[1] E-mail: vmatveev@insti.physics.sunysb.edu.
[2] E-mail: shrock@insti.physics.sunysb.edu.

PII S0375-9601(96)00601-9

physical phase. $\mathcal{B}$ may also include arcs or line segments which protrude into, and terminate in, certain CT phases.

In general, phase boundaries of physical systems include intersection points where different parts of the boundaries meet. Examples include (i) the triple point in the (T,p) phase diagram for a substance like argon, water, etc., where gas, liquid, and solid phases all coexist, and (ii) the two triple points forming the ends of the λ line in the phase diagram for helium, where, at the lower end of this line, the gas, normal fluid and superfluid coexist, and, at the upper end, the solid coexists with the normal fluid and superfluid. Similarly, the complex-temperature phase boundary $\mathcal{B}$ of a spin system may include intersection points at which different curves contained in $\mathcal{B}$ meet. We denote the number of curves meeting at such an intersection point as n_c. Often these can be grouped into pairs, such that two curves meet with equal tangents at the intersection point; these are then regarded as a single branch of a curve passing through this point. In the terminology of algebraic geometry [8], a singular point of an algebraic curve is a multiple (intersection) point of index m if m branches of the curve pass through this point. This is thus an intersection point with $n_c = 2m$ curves meeting, in m pairs with $n_t = m$ equal tangents. For the 2D Ising model on the (homopolygonal) square, triangular, and honeycomb lattices, and also on the heteropolygonal $3 \times 6 \times 3 \times 6$ (kagomé) and $3 \times 12 \times 12$ lattices, the CT phase boundaries $\mathcal{B}$ are algebraic curves and their intersection points always have $n_c = 4$ and $n_t = 2$ so that they are regular multiple points of index $m = 2$ (see Tables 2, 3 in Ref. [9]). This is also true of the Ising model in a nonzero external field satisfying the Lee–Yang condition $\beta H = i\pi/2$; the CT phase boundaries $\mathcal{B}$ on the square, triangular, honeycomb, and $3 \times 12 \times 12$ lattices all exhibit intersection points with $n_c = 4$, $n_t = 2$, which are thus again regular multiple points of index $m = 2$ [10]. In all of these cases, the two branches of the curves cross with an angle $\theta_c = \pi/2$, i.e., orthogonally.

However, in other models, it appears that the respective phase boundaries $\mathcal{B}$ have intersections at finite complex-temperature points with the odd $n_c = 3$. In contrast to the 2D Ising model results noted above, which are extracted (in Refs. [2,5,9,11,12]) from exact solutions (Ref. [14] for square lattice; reviewed for general lattices in Ref. [15]), up to the present time, to our knowledge, none of the models which appear to have finite-K intersection points with odd n_c has been exactly solved (here, $K = J/k_BT$). Instead, the occurrence of such points has been inferred from inspection of CT zeros of the partition function calculated on finite lattices. For example, for the (spin 1/2) Ising model on the simple cubic lattice, such zeros [4,17] suggest an intersection point at $u_{1/2} \simeq -0.5$, where $u_s = e^{-K/s^2}$. At this point, a component of $\mathcal{B}$ crossing the negative real $u_{1/2}$ axis vertically meets a line segment lying on this axis in a T intersection, so that $n_c = 3$, $n_t = 2$. Since the lattice is bipartite, there is a similar intersection point at the inverse position, $u_{1/2} \simeq -2$. Similarly, in our studies of the spin 1 Ising model on the square lattice we have found, for the largest lattice sizes, indications of $n_c = 3$ intersection points at $u_1 \simeq 0.1 + 0.8i$, its inverse, and their complex-conjugates [18]. To gain further insight into this feature of complex-temperature phase boundaries, one is motivated to search for an exactly solvable model which exhibits this behavior. We have succeeded in this; the 1D Z_6 clock model provides to our knowledge the first exactly solvable model with a finite-K intersection point having odd n_c, and we analyze it here.

The Z_N clock model is defined at temperature T by the partition function $Z = \sum_{\{\ell_n\}} e^{-\beta\mathcal{H}}$ with $\beta = (k_BT)^{-1}$ and

$$\mathcal{H} = \sum_{\langle nn' \rangle} E(-\ell_n + \ell_{n'}), \tag{1}$$

where the interaction energy is

$$E(-\ell_n + \ell_{n'}) = -J\cos[2\pi(-\ell_n + \ell_{n'})/N], \tag{2}$$

the site variable is $\ell_n = 0, 1, \ldots, N-1$, and $\langle nn' \rangle$ denotes nearest-neighbor pairs. Equivalently, $E = -JS_n \cdot S_{n'}$, where the angles of the (classical) spins take on the discrete values $S_n = (\cos\theta_n, \sin\theta_n)$ with $\theta_n = 2\pi\ell_n/N$. We use the notation $K = \beta J$ and $u = e^{-K/2}$. We consider the case $N = 6$ here because it provides a simple exactly solvable example of an intersection point with odd n_c on a complex-temperature phase boundary $\mathcal{B}$. The (reduced) free energy is $f = -\beta F = \lim_{N_s\to\infty} N_s^{-1} \ln Z$ in the thermodynamic limit.

For $d = 1$ dimension, one can solve this model exactly, e.g., by transfer matrix methods. One has

$$Z = \mathrm{Tr}(\mathcal{T}^{N_s}) = \sum_{j=1}^{6} \lambda_j^{N_s}, \tag{3}$$

where the λ_j, $j = 1,\ldots,6$ denote the eigenvalues of the transfer matrix $\mathcal{T}$ defined by $\mathcal{T}_{nn'} = \langle \ell_n | \exp[-\beta E(\ell_n, \ell_{n'})] | \ell_{n'} \rangle$, and we use periodic boundary conditions. It is convenient to analyze the phase diagram in the u plane. For physical temperature, phase transitions are associated with degeneracy of leading eigenvalues [16]. There is an obvious generalization of this to the case of complex temperature: in a given region of u, the eigenvalue of $\mathcal{T}$ which has maximal magnitude, $\lambda_{\max}$, gives the dominant contribution to Z and hence, in the thermodynamic limit, f receives a contribution only from $\lambda_{\max}$: $f = \ln(\lambda_{\max})$. For complex K, f is, in general, also complex. The CT phase boundaries are determined by the degeneracy, in magnitude, of leading eigenvalues of $\mathcal{T}$. As one moves from a region with one dominant (i.e., leading) eigenvalue $\lambda_{\max}$ to a region in which a different eigenvalue $\lambda'_{\max}$ dominates, there is a non-analyticity in f as it switches from $f = \ln(\lambda_{\max})$ to $f = \ln(\lambda'_{\max})$. The boundaries of these regions are defined by the degeneracy condition among dominant eigenvalues, $|\lambda_{\max}| = |\lambda'_{\max}|$. These form curves in the u plane. Note that the free energy and the conditions for CT phase boundaries are the same if some eigenvalues occur with finite multiplicity greater than one. To see this, assume λ_j occurs n_j times, where n_j is finite. If λ_j is nonleading, the result is obvious; if λ_j is leading, the result follows because $\lim_{N_s\to\infty} N_s^{-1} \ln(n_j \lambda_j^{N_s}) = \ln \lambda_j$ for any finite (nonzero) n_j. This is relevant here because two of the eigenvalues of $\mathcal{T}$ occur with multiplicity 2.

Of course, a 1D spin model with finite-range interactions has no non-analyticities for any (finite) value of K, so that, in particular, the 1D Z_6 model is analytic along the positive real u axis. Because of the invariance of Z on a bipartite lattice under the transformation $S_e \to S_e$, $S_o \to -S_o$, $J \to -J$, where e and o denote sites on even and odd sublattices, it follows that

$$u \to 1/u \quad \Longrightarrow \quad \mathcal{B} \text{ invariant.} \tag{4}$$

(For a finite 1D lattice with periodic boundary conditions, we preserve this invariance by using even N_s.) Further, since the λ_j are analytic functions of u, whence $\lambda_j(u_s^*) = \lambda_j(u_s)^*$, it follows that the solutions to the degeneracy equations defining the boundaries between different phases, $|\lambda_i| = |\lambda_j|$, are invariant under $u \to u^*$. Hence, $\mathcal{B}$ is invariant under $u \to u^*$.

Although the model has a physical phase structure consisting only of the Z_6-symmetric, disordered phase, its complex-temperature phase diagram is nontrivial and exhibits a number of interesting features. An important property of this model is that the interaction energies $E(\Delta\ell)$, where $\Delta\ell = \ell_n - \ell_{n'}$, are all rational multiples of each other: $E(\Delta\ell)/J = -1, -1/2, 1/2$, and 1 for $\Delta\ell = 0, \pm 1, \pm 2$, and ± 3, respectively, with $E(6 - \Delta\ell) = E(\Delta\ell)$. Hence, all of the Boltzmann weights are powers of $u = e^{-K/2}$. The transfer matrix $\mathcal{T} = \langle \ell_n | e^{-\beta\mathcal{H}} | \ell_{n'} \rangle$ has the Toeplitz form

$$\mathcal{T} = u^{-2} \begin{pmatrix} 1 & u & u^3 & u^4 & u^3 & u \\ u & 1 & u & u^3 & u^4 & u^3 \\ u^3 & u & 1 & u & u^3 & u^4 \\ u^4 & u^3 & u & 1 & u & u^3 \\ u^3 & u^4 & u^3 & u & 1 & u \\ u & u^3 & u^4 & u^3 & u & 1 \end{pmatrix}. \tag{5}$$

The eigenvalues are

$$\lambda_1 = u^{-2} - 2u^{-1} + 2u - u^2 = u^{-2}(1+u)(1-u)^3, \tag{6}$$

$$\lambda_2 = u^{-2} + 2u^{-1} + 2u + u^2 = u^{-2}[1 + (1+\sqrt{3})u + u^2][1 + (1-\sqrt{3})u + u^2], \tag{7}$$

$$\lambda_3 = \lambda_4 = u^{-2} + u^{-1} - u - u^2 = u^{-2}(1-u)(1+u)(1+u+u^2), \tag{8}$$

$$\lambda_5 = \lambda_6 = u^{-2} - u^{-1} - u + u^2 = u^{-2}(1-u)^2(1+u+u^2), \tag{9}$$

and we set $\lambda_{34} \equiv \lambda_3 = \lambda_4$ and $\lambda_{56} \equiv \lambda_5 = \lambda_6$.

We find the complex-temperature phase diagram shown in Fig. 1, consisting of five different phases. In the caption, each phase is labelled by the eigenvalue (or identically equal eigenvalues) which is (are) dominant within it. The first phase is the complex-temperature extension (CTE) of the physical Z_6-symmetric, paramagnetic (PM) phase, denoted R_2 since λ_2 is dominant in this phase. The other four regions have no overlap with any physical phase and are thus of O ("other") type in our previous notation [11]. These include two phases R_{34} and R_{34}^* in which λ_{34} is dominant; these are related to each other by

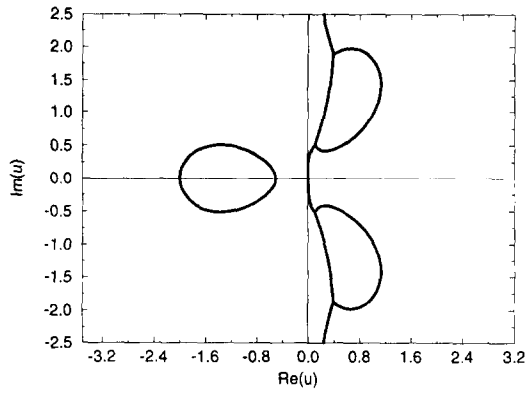

Fig. 1. Phase diagram of the 1D Z_6 clock model in the complex u plane. Phases are (a) R_2 in the $\mathrm{Re}(u) > 0$ half-plane, extending in from the far right; (b) R_{34} occupying the truncated lobe-like region in the northeast quadrant, and its complex conjugate phase, R_{34}^*; (c) R_1 occupying most of the $\mathrm{Re}(u) < 0$ region, and (d) the oval-like phase R_{56} centered on the negative real u axis.

complex conjugation and occupy regions shaped like truncated lobes in the $\mathrm{Re}(u) > 0$ half-plane. Next, there is the phase R_1 which occupies most of the left-hand plane $\mathrm{Re}(u) < 0$ together with a narrow portion to the right of the vertical axis $\mathrm{Re}(u) = 0$. The fifth phase, R_{56} comprises an oval-like region centered on the negative real u axis in which λ_{56} is dominant. A striking feature of the CT phase diagram is the presence of four intersection points on the CT boundary $\mathcal{B}$, at $u \simeq 0.11 + 0.51\mathrm{i}$ (given more precisely below), its inverse, and their complex conjugates. This is quite different from the CT phase diagram for the 1D higher-spin Ising model [19], where the curves (and, for half-integral spin, the semi-infinite line segment on the negative real u_s axis) only meet at the origin of the complex u_s plane, i.e., at $K = \infty$, where the model has an FM critical point and a formal essential singularity. This intersection point has $n_c = 4s^2$. (Given the $u \to 1/u$ in the latter model, in the u_s^{-1} plane, the curves also meet at the AFM critical point at $u_s^{-1} = 0$.) A further difference is the presence in the Z_6 model of CT phases of finite extent in the u plane, viz., R_{34}, R_{34}^*, and R_{56}. In the 1D spin s Ising model, all CT phases extend from the wedge which they occupy in the vicinity of the origin outward to the circle at infinity in the u_s plane. A third comparison may be made with the CT phase diagram for the 1D q-state Potts model, which has no intersection points on $\mathcal{B}$ and, for $q \geq 3$, just two phases in the e^{-K} plane, the CT extension of the PM phase, of infinite extent, and an O phase of finite extent, bounded by the circle $e^{-K} = (-1 + e^{i\omega})/(q-2)$ [19]. (The $q = 2$ Potts model is equivalent to the spin 1/2 Ising model.)

To discuss the CT phase diagram of the 1D Z_6 model, we consider first the oval boundary of the phase R_{56}. This is the simplest portion of $\mathcal{B}$ because it does not contain any intersection points. It is the locus of solutions to the degeneracy condition $|\lambda_1| = |\lambda_{56}|$ where these alternate as the dominant eigenvalues. Let $u = re^{i\theta}$. Then

$$|\lambda_1| = |\lambda_{56}| \implies r[r + 2(1+r^2)\cos\theta + 4r\cos 2\theta] = 0. \qquad (10)$$

Note that in obtaining the equation in r and θ above from the condition $|\lambda_1| = |\lambda_{56}|$, we have removed the common factor $|1-u|^2$, which is irrelevant for $\mathcal{B}$, since at $u = 1$ the condition that λ_1 and λ_{56} are dominant is not satisfied (indeed, both vanish there). Further, in Eq. (10), the solution $r = 0$, i.e. $u = 0$, is not relevant for $\mathcal{B}$, since λ_{56} is not a dominant eigenvalue at this point. Equating the remaining factor to zero in the region where λ_1 and λ_{56} alternate as dominant eigenvalues, one obtains the oval curve shown in Fig. 1. (If one relaxes the condition that λ_1 and λ_{56} be dominant eigenvalues, then one obtains also a curve in the $\mathrm{Re}(u) \geq 0$ half-plane passing through $u = 0$, extending in "northeast" and "southeast" directions; however, this is not relevant for $\mathcal{B}$.) Equating the factor in square brackets in Eq. (10) to zero and solving, one gets

$$\cos\theta_{1-56,\pm} = \tfrac{1}{8}[-(r^{-1}+r) \pm \sqrt{r^{-2}+26+r^2}]. \qquad (11)$$

Observe the $r \to 1/r$ symmetry in (11), in accord with (4). The $-$ sign gives the oval while the $+$ sign gives the above-mentioned curve in the $\mathrm{Re}(u) \geq 0$ region, which does not contribute to $\mathcal{B}$. Setting $\theta = \pi$ in (10) yields the solutions $r = 1/2$ and $r = 2$, i.e. $u = -1/2$ and $u = -2$; these are the points where the oval boundary crosses the negative real u axis. Setting $r = 1$ in the $-$ case of Eq. (11) yields the values of θ at which the oval boundary crosses the unit circle $|u| = 1$, which are given by $\pm\theta_0$, where

$$\theta_0 = \arccos\left(-\frac{1+\sqrt{7}}{4}\right) = 155.705°. \qquad (12)$$

The corresponding points are

$$\tfrac{1}{4}[-(1+\sqrt{7}) \pm (8-2\sqrt{7})^{1/2}] \simeq -0.911 \pm 0.411\mathrm{i}. \quad (13)$$

As one travels along the boundary curve of the oval, θ starts at the value π at $u = -1/2$, decreases to the value θ_0 as u crosses the unit circle, and then increases back to $\theta = \pi$ at $u = -2$, and similarly with the complex conjugate points.

The portion of $\mathcal{B}$ in the $\mathrm{Re}(u) \geq 0$ half-plane is more complicated and consists of several parts, each of which represents a degeneracy condition of the form $|\lambda_i| = |\lambda_j|$ where λ_i and λ_j alternate as dominant eigenvalues. The part of $\mathcal{B}$ near the origin (and hence also, given the symmetry (4), the part farthest out from the origin) is a curve consisting of the solution to the condition

$$|\lambda_1| = |\lambda_2| \implies r[2(1+r^6)\cos\theta + 4r^3\cos 2\theta + r^3\cos 4\theta] = 0, \quad (14)$$

where λ_1 and λ_2 are dominant eigenvalues. For $r \neq 0$, we analyze the second factor in square brackets. For small r this reduces to the condition that $\cos\theta = 0$, i.e., $\theta = \pm\pi/2$, so that this curve passes through the origin in a vertical direction. (Eq. (14) also has a solution consisting of a small oval which crosses the negative real u axis at $-2^{\pm 1/3}$, but this is not relevant to $\mathcal{B}$ since λ_1 and λ_2 do not alternate as dominant eigenvalues in this region.)

The left-hand boundaries of the lobe regions R_{34} and R_{34}^* are given by the solution to the condition

$$|\lambda_1| = |\lambda_{34}| \implies r[r - 2(1+r^2)\cos\theta] = 0, \quad (15)$$

i.e., $\cos\theta = r/2(1+r^2)$, where these eigenvalues are dominant. The corresponding curve crosses the unit circle at $\theta = \arccos(1/4) \simeq \pm 75.52°$.

The right-hand boundaries of these lobe regions R_{34} and R_{34}^* are given by the solution to the condition

$$|\lambda_2| = |\lambda_{34}| \implies r[3r(1+r^4) + 2(1+r^6)\cos\theta + 10r^3\cos 2\theta + 6r^2(1+r^2)\cos 3\theta + 4r^3\cos 4\theta] = 0, \quad (16)$$

where λ_2 and λ_{34} alternate as dominant eigenvalues. This curve crosses the unit circle at $\cos\theta = a^{1/3} + (3/8)a^{-1/3} - 1/2$, where $a = (9+3\sqrt{3})/32$, i.e., $\theta = \pm 41.03°$.

As noted above, there are four intersection points, each with $n_c = 3$, on $\mathcal{B}$. We denote the one closest to the origin in the northeast quadrant as $u_t = r_t e^{i\theta_t}$; the others are then $1/u_t$, and their complex conjugates, u_t^* and $1/u_t^*$. The point u_t occurs where the three eigenvalues λ_1, λ_2, and λ_{34} are all degenerate and dominant, i.e., where the phase boundaries defined by the conditions $|\lambda_1| = |\lambda_2|$, $|\lambda_1| = |\lambda_{34}|$, and $|\lambda_2| = |\lambda_{34}|$ all meet. This point is given by the solution $r_t = 0.518684\ldots$ to the equation

$$2(r^{-6} + r^6) - 18(r^{-2} + r^2) - 31 = 0. \quad (17)$$

This equation is manifestly symmetric under the symmetry (4), and has two positive real reciprocal roots, of which the smaller is the one which we have listed above. The corresponding angle is $\theta_t = 78.207851°$, so that

$$u_t \simeq 0.1059993 + 0.5077375\mathrm{i}. \quad (18)$$

A general characteristic of 1D spin models with short-range forces is that the points $K = \pm\infty$ are critical points, so that in the present case, the phase boundary $\mathcal{B}$ passes through the respective origins in the u and u^{-1} planes. This is reminiscent of how $\mathcal{B}$ passed through the origin of the u_s plane for the 1D spin s Ising model and the e^{-K} plane for the 1D q-state Potts model [19].

In order to gain further insight into the components of $\mathcal{B}$, one may determine the full locus of points comprising the solution of the degeneracy condition $|\lambda_i| = |\lambda_j|$ without the constraint that λ_i and λ_j be dominant eigenvalues. One can then see how subsets of this locus form the various components of $\mathcal{B}$. In Fig. 2 we show the portions of the solutions to the $|\lambda_i| = |\lambda_j|$ equations for $(i,j) = (1,2)$, (1,34), and (2,34) which are involved with the finite-K intersection points. The loci of solutions to $|\lambda_2| = |\lambda_{34}|$ and $|\lambda_1| = |\lambda_{56}|$ also contain curves which pass through the origins of the u and u^{-1} planes; we omit these from Fig. 2 since they do not contribute to $\mathcal{B}$ except at the respective origins of the u and u^{-1} planes, which are the zero-temperature FM and AFM critical points of the model. The intersection point u_t, together with its inverse and their complex conjugates, are seen to be the (finite-K) points at which all of the curves $|\lambda_i| = |\lambda_j|$ for

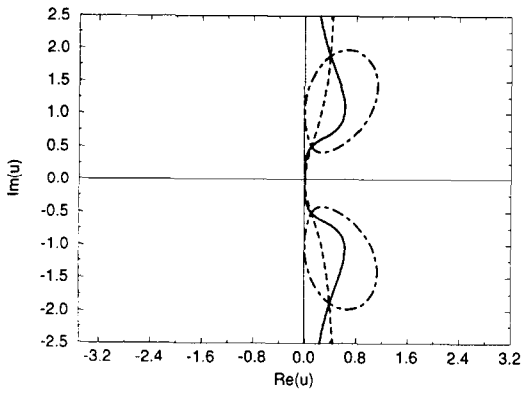

Fig. 2. Solutions with $\mathrm{Re}(u) \geq 0$ of the conditions (a) $|\lambda_1| = |\lambda_2|$ (solid curve); (b) $|\lambda_1| = |\lambda_{34}|$ (dashed curve); and (c) $|\lambda_2| = |\lambda_{34}|$ (dot-dashed curve).

$(i,j) = (1,2)$, $(1,34)$, and $(2,34)$ cross. While a solution curve of $|\lambda_i| = |\lambda_j|$ for a given (i,j) continues smoothly through u_t, the actual CT phase boundary $\mathcal{B}$ has a discontinuous tangent there and heads off in a different direction as one moves away from u_t, since it is then determined by a different degeneracy condition $|\lambda_j| = |\lambda_k|$.

We generalize our results as follows: for a 1D discrete spin model with short-ranged interactions, so that the transfer matrix has a finite number of eigenvalues, the CT phase boundary $\mathcal{B}$ has an intersection point with n_c curves meeting if and only if n_c (in general distinct) dominant eigenvalues become degenerate in magnitude at this point.

Of course, there are differences between $d = 1$ and $d \geq 2$ models. For $d \geq 2$, $\mathcal{T}$ has an infinite number of eigenvalues, rather than the finite number which it has for $d = 1$. Further, since $d > 1$ is above the lower critical dimensionality $d_{\mathrm{l.c.d.}} = 1$ of a usual discrete spin model, two eigenvalues which are distinct in the symmetric phase may be degenerate in the phase with spontaneously broken symmetry and ferromagnetic (FM) or antiferromagnetic (AFM) long-range order, again in contrast to the situation in $d = 1$, where there is no symmetry-breaking phase for finite K. However, these differences do not prevent the 1D Z_6 model from having the same feature, viz., an intersection point on $\mathcal{B}$ with $n_c = 3$, as higher-dimensional models such as the spin 1/2 3D Ising model.

Indeed, we have previously pointed out some intriguing connections between certain features of the respective CT phase boundaries of the higher-spin Ising model in 1D and 2D [18,19]. These included the observation that (exactly known) angles at which phase boundaries crossed the unit circle in the 1D case were consistent with being equal to values of analogous angles in the 2D model. Remarkably, we find the same kind of connection here. The physical phase structure of the 2D Z_6 model consists of (i) a disordered, Z_6-symmetric high-temperature phase, (ii) a Z_6-symmetric intermediate-temperature phase with algebraic decay of correlations, and (iii) a broken-symmetry low-temperature phase with FM (AFM) long-range order for $J > 0$ ($J < 0$) [20]. From the CT zeros of the partition function for the Z_6 model calculated on a 6×7 lattice [21], which we have confirmed in an independent calculation, one infers that in the "northwest" and "southwest" regions of the u plane, in the thermodynamic limit, $\mathcal{B}$ has intersection points with $n_c = 4$, $n_t = 2$, and $m = 2$ at $e^{\pm i\theta_0}$, where θ_0 is the same angle as we have calculated in Eq. (12). This suggests that one can gain valuable information about certain features of the complex-temperature properties of a higher-dimensional spin model from the CT properties of the corresponding 1D model, reminiscent of the fact that ϵ expansions starting from $d = d_{\mathrm{l.c.d.}}$ gave similar insight into the physical phase transition in models for $d > d_{\mathrm{l.c.d.}}$ [22].

This research was supported in part by the NSF grant PHY-93-09888.

References

[1] C.N. Yang and T.D. Lee, Phys. Rev. 87 (1952) 404;
T.D. Lee and C.N. Yang, Phys. Rev. 87 (1952) 410.
[2] M.E. Fisher, Lectures in theoretical physics, Vol. 7C (Univ of Colorado Press, 1965) p. 1.
[3] S. Katsura, Prog. Theor. Phys. 38 (1967) 1415;
Y. Abe and S. Katsura, Prog. Theor. Phys. 43 (1970) 1402.
[4] S. Ono, Y. Karaki, M. Suzuki and C. Kawabata, J. Phys. Soc. Japan 25 (1968) 54.
[5] R. Abe, Prog. Theor. Phys. 38 (1967) 322.
[6] C. Kawabata and M. Suzuki, J. Phys. Soc. Japan 27 (1969) 1105.
[7] C.J. Thompson, A.J. Guttmann and B.W. Ninham, J. Phys. C 2 (1969) 1889;
A.J. Guttmann, J. Phys. C 2 (1969) 1900;
C. Domb and A.J. Guttmann, J. Phys. C 3 (1970) 1652.
[8] S. Lefschetz, Algebraic geometry (Princeton Univ. Press, Princeton, 1953);
R. Hartshorne, Algebraic geometry (Springer, Berlin, 1977).

[9] V. Matveev and R. Shrock, J. Phys. A 28 (1995) 5235.
[10] V. Matveev and R. Shrock, J. Phys. A 28 (1995) 4859; Phys. Rev. E 53 (1996) 254.
[11] V. Matveev and R. Shrock, J. Phys. A 28 (1995) 1557.
[12] V. Matveev and R. Shrock, J. Phys. A 29 (1996) 803.
[13] R. Abe, T. Dotera and T. Ogawa, Prog. Theor. Phys. 85 (1991) 509.
[14] L. Onsager, Phys. Rev. 65 (1944) 117.
[15] C. Domb, Adv. in Phys. 9 (1960) 149;
I. Syozi, in: Phase transitions and critical phenomena, Vol. 3, eds. C. Domb and M.S. Green (Academic Press, New York, 1972) p. 269.
[16] J. Ashkin and W.E. Lamb, Phys. Rev. 64 (1943) 159.
[17] R.B. Pearson, Phys. Rev. B 26 (1982) 6285;
C. Itzykson, R.B. Pearson and J.B. Zuber, Nucl. Phys. B 220 (1983) 415.
[18] V. Matveev and R. Shrock, J. Phys. A 28 (1995) L533.
[19] V. Matveev and R. Shrock, Phys. Lett. A 204 (1995) 353.
[20] S. Elitzur, R.B. Pearson and J. Shigemitsu, Phys. Rev. D 19 (1979) 3698.
[21] P.P. Martin, J. Phys. A 21 (1988) 4415; Potts models and related problems in statistical mechanics (World Scientific, Singapore, 1991).
[22] A.A. Migdal, Zh. Eksp. Teor. Fiz. 69 (1975) 1457 [JETP 42 (1975) 743];
A.M. Polyakov, Phys. Lett. B 59 (1975) 79;
E. Brézin and J. Zinn-Justin, Phys. Rev. Lett. 36 (1976) 691; Phys. Rev. B 14 (1976) 3110;
W.A. Bardeen, B.W. Lee and R.E. Shrock, Phys. Rev. D 14 (1976) 985.